Small-volume waveguide-section high *Q* microcavities in 2D photonic crystal slabs

Ziyang Zhang and Min Qiu

Laboratory of Optics, Photonics and Quantum Electronics,
Department of Microelectronics and Information Technology,
Royal Institute of Technology (KTH),
Electrum 229, 164 40 Kista, Sweden,
min@imit.kth.se

Abstract: A series of microcavities in 2D hexagonal lattice photonic crystal slabs are studied in this paper. The microcavities are small sections of a photonic crystal waveguide. Finite difference time domain simulations show that these cavities preserve high *Q* modes with similar geometrical parameters and field profile. Effective modal volume is reduced gradually in this series of microcavity modes while maintaining high quality factor. Vertical *Q* value larger than 10^6 is obtained for one of these cavity modes with effective modal volume around *5.40* cubic half wavelengths $[(\lambda/2n_{slab})^3]$. Another cavity mode provides even smaller modal volume around *2.30* cubic half wavelengths, with vertical *Q* value exceeding10^5.

OCIS codes: (230.5750) Resonators; (230.3990) Microstructure devices

References and links

1. E. Yablonovitch, "Inhibited Spontaneous Emission in Solid-State Physics and Electronics," Phys. Rev. Lett. **58**, 2059 (1987)
2. S. John, "Strong localization of photons in certain disordered dielectric superlattices," Phys. Rev. Lett. **58**, 2486 (1987)
3. H. Benisty, "Modal analysis of optical guides with two-dimensional photonic band-gap boundaries," J. Appl. Phys. **75**, 4753 (1994)
4. A. Mekis, S. Fan, and J. D. Joannopoulos, "Bound states in photonic crystal waveguides and waveguide bends", Phys. Rev. B **58**, 4809 (1998)
5. T. F. Krauss, R. M. De La Rue, and S. Brand, "Two-dimensional photonic-bandgap structures operating at near-infrared wavelengths", Nature **383**, 699 (1996)
6. S. G. Johnson, S. Fan, P. R. Villeneuve, J. D. Joannopoulos, and L. A. Kolodziejski, "Guided modes in photonic crystal slabs," Phys. Rev. B, **60**, 5751 (1999)
7. S. Fan, Pierre R. Villeneuve, and J. D. Joannopoulos, "Channel Drop Tunneling through Localized States," Phys. Rev. Lett. **80**, 960 (1998)
8. M. Qiu, "Ultra-compact optical filter in two-dimensional photonic crystal," Electron. Lett. **40**, 539 (2004)
9. M. Qiu and B. Jaskorzynska, "A design of a channel drop filter in a two-dimensional triangular photonic crystal", Appl. Phys. Lett. **83**, 1074 (2003).
10. S. Fan, Proceedings of the SPIE, **v 3002**, 1997, p 67-73
11. Spillane, S. M., Kippenberg, T. J. and Vahala, K. J. "Ultralow-threshold Raman laser using a spherical dielectric microcavity," S. M. , Nature **415**, 621-623 (2002)
12. P. Michler, A. Kiraz, C. Becher, W. V. Schoenfeld, P. M. Petroff, Lidong Zhang, E. Hu, and A. Imamoglu, "Quantum Dot Single-Photon Turnstile Device," Science **290**, 2282 (2000)
13. C. Santori, D. Fattal, J. Vuc˘kovic´ , G. S. Solomon, and Y. Yamamoto, "Indistinguishable photons from a single-photon device," Nature **419**, 594 (2002)
14. K. Srinivasan and O. Painter, "Momentum space design of high-Q photonic crystal optical cavities," Opt. Express **10**, 670 (2002), http://www.opticsexpress.org/abstract.cfm?URI=OPEX-10-15-670
15. J. Vučković, M. lončar, H. Mabuchi and A. Scherer, "Optimization of the Q factor in photonic crystal microcavities," IEEE J. of Quantum Electron. **38**, 850 (2002)
16. K. Srinivasan and O. Painter, "Fourier space design of high-Q cavities in standard and compressed hexagonal lattice photonic crystals," Opt. Express **11**, 579 (2003), http://www.opticsexpress.org/abstract.cfm?URI=OPEX-11-6-579
17. V. Akahane, T. Asano, B. S. Song, and S. Noda, "High-Q photonic nanocavity in a two-dimensional photonic crystal," Nature **425**, 944 (2003)

#4784 - $15.00 US Received 12 July 2004; revised 9 August 2004; accepted 10 August 2004

18. H. Y. Ryu, M. Notomi, and Y. H. Lee, "High-quality-factor and small-mode-volume hexapole modes in photonic-crystal-slab nanocavities," Appl. Phys. Lett. **83**, 4294 (2003)
19. E.Yablonovitch and T. J. Gmitter, "Donor and acceptor modes in photonic band structure," Phys. Rev. Lett. **67**, 3380 (1991)
20. K. S. Yee, "Numerical solution of initial boundary value problems involving Maxwell's equations in isotropic media," IEEE Trans. Antennas and Propagation," **14**, 302 (1966)
21. J. P. Berenger, "A perfectly matched layer for the absorption of electromagnetic waves," J. Comput. Phys. **114**, 185 (1994)
22. M. Qiu, "High Q cavities in photonic crystal slabs: determining resonant frequency and quality factor accurately," submitted for publication (2004)
23. W. H. Guo, W. J. Li, and Y. Z. Huang, "Computation of Resonant Frequencies and Quality Factors of Cavities by FDTD Technique and Padé Approximation," IEEE Microwave Wireless Components Lett. **11**, 223 (2001)
24. O. Painter, R. K. Lee, A. Scherer, A. Yariv, J. D. O'Brien, P. D. Dapkus, and I. Kim, "Two-Dimensional Photonic Band-Gap Defect Mode Laser," Science **284**, 1819 (1999)
25. J. Vučković, M. lončar, H. Mabuchi and A. Scherer, "Design of photonic crystal microcavities for cavity QED," Phys. Rev. E. **65**, 016608 (2001)

1. Introduction

The discovery of photonic crystals has opened up many new methods to manipulate light [1-2]. However, three dimensional photonic crystals usually involves complex connectivity and strict alignment, which make them rather challenging for fabrication [3-4]. Alternatively, two dimensional photonic crystal slabs (2D PCS's) have been proposed [5-6], which promise easier fabrication using present techniques.

Over the past few years, much work has been devoted to the study of microcavities in these 2D PCS's. These microcavities exhibit attractive properties such as high quality factor (Q) and small modal volume (V), which make them potentially useful not only in miniaturized photonic devices but also in some quantum optical devices. The former applications include channel drop filter for the wavelength division multiplexer system, high efficiency light emission diodes and low threshold lasers [7-11]. Among the latter applications are controlled single photon source and entangled emitter-cavity systems [12-13].

The applications mentioned above all require microcavities to confine light strongly and densely, that is, microcavities should have both high quality factor Q and small modal volume V. The ratio Q/V is a measure of the strength of various cavity interactions and should be as large as possible.

There have been many theoretical and experimental studies to improve the quality factor of microcavities in 2D PCS's. It is known that total Q value (Q_{tot}) can be separated into two parts, namely the in-plane Q value ($Q_{\parallel}$) and the vertical Q value ($Q_{\perp}$) by a simple relation $\frac{1}{Q_{tot}} = \frac{1}{Q_{\parallel}} + \frac{1}{Q_{\perp}}$. In a 2D PCS microcavity, light is confined within the defect region by two combined mechanisms, namely distributed Bragg reflection (in-plane) and total internal reflection (vertically). The in-plane confinement is determined by the number of periods of the host lattice surrounding the cavity, with the assumption that the resonant frequency of the defect mode lies within the in-plane guided mode bandgap. Thus, the more periods surrounding the defect, the stronger the in-plane light confinement and the larger the in-plane Q value ($Q_{\parallel}$). The vertical confinement is due to the standard waveguiding by total internal reflection. In momentum ($\boldsymbol{k}$) space analysis, vertical radiation losses occur when the cavity modes have in-plane momentum components ($\boldsymbol{k}_{\parallel}$) that lie within a region called 'light cone' [14-15]. The larger the fraction of in-plane momentum components that lie within this light cone, the larger the vertical radiation loss and consequently the smaller the vertical Q value.

#4784 - $15.00 US Received 12 July 2004; revised 9 August 2004; accepted 10 August 2004

As we have seen, one of the key issues in the design of high Q microcavity in 2D PCS's is to reduce the $\boldsymbol{k}_{\triangleleft}$ field components that lie within the light cone and thus enhance the vertical confinement. One group has achieved this by carefully modifying the air hole radii into a graded pattern [16]. This leads to some cavity modes with $Q_{\perp}$ larger than 10^5. Another group has come up with a design of simpler structure [17]. The cavity is constructed by removing three air holes in a row and shifting the left, right adjacent holes outwards by $0.15\,a$, where a is the lattice constant. Experiments have shown that the cavity supports a resonant mode with a high quality factor $Q = 4.5\times10^4$ and a small modal volume $V = 7.0\times10^{-14}\,cm^3$. Recently a group has reported a hexapole cavity mode with Q larger than 10^6 and small modal volume on the order of cubic wavelengths in material [18]. However, this high Q hexapole mode is very sensitive to its surrounding geometrical parameters, which might bring up difficulties for fabrication.

In this paper, we start with a cavity similar to that in Ref. [17], but consider it as a short section of a line defect (waveguide), ended with perfect 2D photonic crystal lattices (as shown in Fig. 1). We shorten this waveguide section gradually to reduce the modal volume and study how its Q value varies. Contrary to the acceptor mode in Ref. [17], whose resonant frequency lies slightly above the lower bandedge [19], we concentrate on the donor mode inside this encapsulated waveguide section cavity that has a higher resonant frequency just below the upper bandedge.

The paper is organized as follows: We first introduce the methods we use, including the setup for the finite difference time domain (FDTD) simulations, how to calculate Q value and effective modal volume. In section 3, we begin with a three missing hole cavity (named as an M3 cavity). We first modify its surrounding geometrical parameters to achieve highest Q value for this mode and then calculate its modal volume. Next, we run the same procedures on two missing hole cavities (M2), one missing hole cavities (M1) and finally cavities with no missing hole at all (M0). In section 4, we give a brief comparison of the cavity modes.

2. Calculation methods

We use the finite difference time domain method for our simulations [20]. The structure size is $23a\times23a$ for the entire cavity modes calculated in this paper, which is capable of providing sufficiently large $Q_{\triangleleft}$ so that Q_{tot} is primarily limited by $Q_{\perp}$. The grid size is $0.05a$ in x, z direction and $0.0433a$ in y direction. Perfect matched layers are used as absorbing boundaries [21].

The Q_{tot} value of the cavity modes is calculated using a combination of FDTD techniques and Padé approximation with Baker's algorithm [22-23], which is capable of achieving ultra accurate Q value using a much smaller number of time steps compared to other methods (typically $<0.5\%$ numerical errors and $\sim15{,}000$ time steps for $Q>10^5$). For comparison reasons, some high Q values of certain cavity modes are also calculated using conventional method: $Q = 2\pi \cdot f_0 \dfrac{U}{P}$, where f_0 is the resonant frequency of the cavity mode, U is the time averaged energy stored in the cavity, and P is the power loss. $Q_{\perp}$ and $Q_{\triangleleft}$ are calculated separately using this method.

The modal volume is calculated using the following equation [24],

$$V = \frac{\iiint \varepsilon(x,y,z)\cdot\left|E(x,y,z)\right|^2 dxdydz}{\max[\varepsilon(x,y,z)\cdot\left|E(x,y,z)\right|^2]}, \tag{1}$$

where $\varepsilon(x,y,z)$ is the spatial distribution of dielectric constant and

$$\left|E(x,y,z)\right|^2 = \left|E_x(x,y,z)\right|^2 + \left|E_y(x,y,z)\right|^2 + \left|E_z(x,y,z)\right|^2. \tag{2}$$

#4784 - $15.00 US Received 12 July 2004; revised 9 August 2004; accepted 10 August 2004

3. Waveguide-section microcavities

3.1 Three missing hole waveguide-section cavity (M3)

The structure of our 2D PCS cavity is shown in Fig. 1, with three missing holes in the center. The refractive index of the slab is chosen to be 3.4, which corresponds to silicon at *1.55* μ*m*. The thickness of the slab is *0.7a*, where *a* is the lattice constant. The radius of the air holes is set to be *R=0.29a*. These two parameters are also the same for M2, M1 and M0 cavities.

As mentioned earlier, we have to reduce the $\boldsymbol{k}_{\sphericalangle}$ components of the cavity mode that lie inside the leaky region in order to achieve high *Q* value. The first step we take is similar to that described in Ref. [16]. Basically, we apply symmetries to enforce special boundary conditions on the momentum space representation of the mode, so that the in-plane electric field polarizations at $\boldsymbol{k}_{\perp} = 0$ (DC) are eliminated. Since all the cavities in this paper support multiple modes, we confine our discussion only to the donor modes whose $\boldsymbol{H}_z$ field distribution is even in both *x* and *y* direction. These modes, as we shall see later, can achieve extremely high Q and ultra small modal volume when the waveguide section is well shortened.

To further reduce the in-plane momentum components inside the leaky region, we modify the geometries of the lattice structure surrounding the defect. This, in essence, changes the Bragg reflection conditions at the cavity edges. By doing so, we allow the light to penetrate deeper inside the surrounding lattice and be reflected gently and perfectly. The spatial variation of the envelope function is tailored into a Gaussian profile, which significantly reduces the momentum components in the leaky region while keeping the modal volume small [17]. As shown in Fig. 1(b), we modify the two geometrical parameters *d* and R_1 to improve the *Q* value.

For simplicity's concern, we will use the same name (M3, M2 and etc.) for the cavity and its donor mode discussed in this paper, although all these cavities support multiple modes.

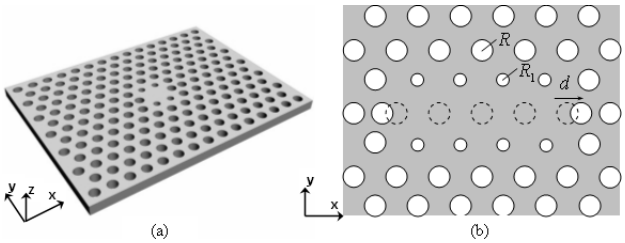

Fig. 1. Schematic diagram of 2D PCS microcavities with three central holes missing in a row. The refractive index of the slab is 3.4 and the thickness t is 0.7*a*. *d* and R_1 are varied to find the largest *Q* of the M3 mode.

After careful scanning of *d* and R_1, we find the highest *Q* value *8,000* can be achieved at *d=0.24a* and R_1*=0.23a*. Figure 2(a) shows the $\boldsymbol{H}_z$ field distribution of the M3 mode. The field is spread out into the surrounding lattice of the cavity and since the resonant frequency *0.3077 a/*λ is near to the upper bandedge (*~0.32 a/*λ), the in-plane quality factor $Q_{\sphericalangle}$ is limited to *35,000* even for a large size (*23a*×*23a*).

For the $\boldsymbol{k}$ space analysis, we take the 2D ($\boldsymbol{k}_x$, $\boldsymbol{k}_y$) Fourier transform of E_x, E_y and H_x, H_y field distribution in the air layer one FDTD grid cell above the slab surface, denoted by $FT_2(E_x)$, $FT_2(E_y)$, $FT_2(H_x)$ and $FT_2(H_y)$, respectively. The total radiated power *P* of the cavity mode can be estimated by the following equations [15].

$$P = \frac{\eta}{8\lambda^2 k^2} \iint_{k_{\parallel} \le k} I \cdot dk_x \cdot dk_y, \tag{3}$$

#4784 - $15.00 US Received 12 July 2004; revised 9 August 2004; accepted 10 August 2004

where $\eta = \sqrt{\frac{\mu_0}{\varepsilon_0}}, k = \frac{2\pi}{\lambda}$, and

$$I = \left| FT_2(H_y) + \frac{1}{\eta} FT_2(E_x) \right|^2 + \left| FT_2(H_x) - \frac{1}{\eta} FT_2(E_y) \right|^2 \quad (4)$$

The distribution of I is shown in Fig. 2(b). We can see that there is still a considerable amount of $\boldsymbol{k}_{\triangleleft}$ component lying inside the light cone, which limits $Q_{\perp}$ to about *10,000*. Using Eqs. (1) and (2), the modal volume V is calculated to be $7.90(\lambda/2n_{slab})^3$ for the M3 mode.

The M3 mode is not very exciting compared to the acceptor mode in Ref. [17], which has $Q_{tot}=9.91\times10^4$ at resonant frequency *0.2618 a/λ* when *d=0.2a* and slab thickness *t=0.6a*, according to our simulations. For *d=0.2a* and *t=0.7a*, Q_{tot} *equals* 2.16×10^4 with resonant frequency *0.2549 a/λ*. However, the donor mode becomes interesting when the waveguide-section is further shortened. Next, we study cavities with only two air holes removed but its surrounding geometrical structures retained.

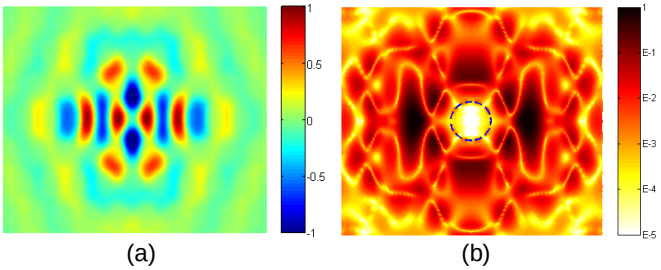

Fig. 2. (a) $\boldsymbol{H}_z$ field distribution of the M3 mode. (b) $\boldsymbol{k}$ space intensity profile *I*. The region inside the blue dashed circle (the light line) is the leaky region.

3.2 Two missing hole waveguide-section cavity (M2)

For the two missing hole cavity, shown in Fig. 3(a), we tune *d=0.23a* and R_1*=0.2a*. Q_{tot} is calculated to be 5.4×10^4, with $Q_{\perp}=6.0\times10^4$ and $Q_{\triangleleft}=4.5\times10^5$. Both $Q_{\perp}$ and $Q_{\triangleleft}$ are much improved compared to the previous case. The former improvement is due to the reduced $\boldsymbol{k}$ space components inside the leaky region, as shown in Fig. 3(c) and the latter improvement is due to the reduced resonant frequency at *0.2955 a/λ*, which is now lying closer to the middle of the bandgap.

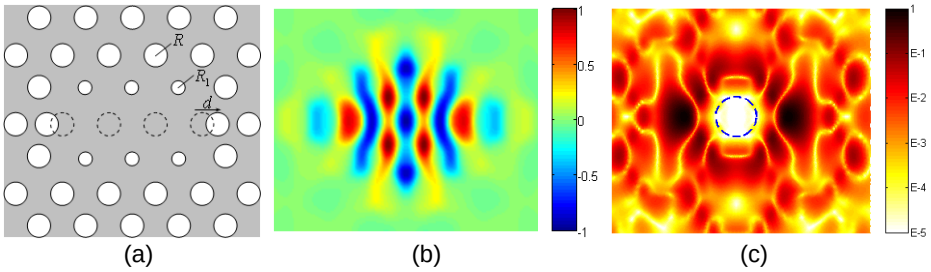

Fig. 3. (a) M2 cavity, with *d=0.23a* and R_1*=0.2a*. (b) $\boldsymbol{H}_z$ field distribution of the M2 mode. (c) $\boldsymbol{k}$ space intensity profile *I*. Components inside the leaky region are reduced compared to the M3 mode in Fig. 2(b)

For the M2 mode, the effective modal volume is calculated to be $9.52\ (\lambda/2n_{slab})^3$.

#4784 - $15.00 US
Received 12 July 2004; revised 9 August 2004; accepted 10 August 2004

3.3 One missing hole waveguide-section cavity (M1)

To further reduce the modal volume, we move on to M1 cavity with only one missing hole, shown in Fig. 4(a). As with the M3 and M2 cavities, we vary d and R_1 to search for the setup of the highest Q donor mode for the M1 cavity. We find when d is tuned to $0.21a$ and R_1 to $0.22a$, $Q_{tot}=5.85\times10^5$ can be achieved at resonant frequency $0.2902\ a/\lambda$. Since M1 cavity is more compact, we vary more geometrical parameters hoping to improve the Q value. We find that by modifying the radius of four air holes from $R=0.29a$ to $R_2=0.25a$ [also shown in Fig. 4(a)], we can largely enhance the Q value for the M1 mode to $Q_{tot}\approx Q_{\perp}=1.06\times10^6$ and $Q_{\measuredangle}>2\times10^7$. The Resonant frequency is further reduced to $0.2881\ a/\lambda$ and modal volume reduced to $5.40\ (\lambda/2n_{slab})^3$.

It is interesting to note that M3, M2 and M1 modes all reach their highest Q value when d and R_1 are tuned to around $0.22a$. We can conclude that tuning d to around $0.22a$ allows light to penetrate deeper inside the surrounding lattice in the x direction and be reflected gently. Similarly, tuning R_1 (and also R_2 for M1 cavity) allows the reflections in the y direction to be smoother. The combined effect is that the spatial variation of the envelope function is tailored into a Gaussian profile so that the $\boldsymbol{k}_{\measuredangle}$ components inside the light cone are reduced and thus $Q_{\perp}$ improved. On the other hand, increasing d and decreasing R_1 helps pull down the resonant frequency closer to the middle of the bandgap [14], which causes $Q_{\measuredangle}$ to increase.

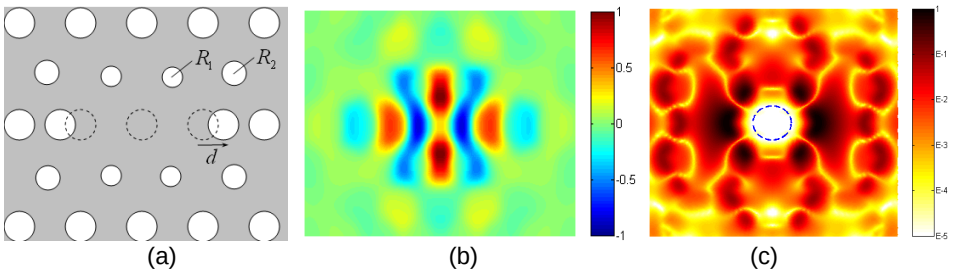

Fig. 4. (a) M1 cavity, with $d=0.21a$, $R_1=0.22a$ *and* $R_2=0.25a$ (b) $\boldsymbol{H_z}$ field distribution of the M1 mode. (c) $\boldsymbol{k}$ space intensity profile I. Components inside the leaky region are greatly reduced compared to the M2 mode in Fig. 3(c)

3.4 Zero missing hole waveguide-section cavity (M0)

There is still room to further reduce the modal volume. We move on to M0 cavity, which involves no missing holes at all. The geometric structure is shown in Fig. 5(a). The structure is very simple, with only two adjacent holes (labeled 'A') shifted outward in x direction by a distance of d and the radius of the two air holes nearest to the cavity center in the y direction (labeled 'B') is modified to R_1. After careful scanning, we find that $d=0.14a$ and $R_1=0.27a$ gives the highest Q. We also modified other geometric parameters, such as the radius of the 'A' holes and the 'C' holes, but this only reduces the Q value of the M0 mode, so we have skipped them in this paper. The final Q value is 1.35×10^5 with resonant frequency $0.2888\ a/\lambda$.

The $\boldsymbol{H_z}$ field distribution is shown in Fig. 5(b). The $\boldsymbol{H_z}$ field profile is now very simple and the number of the nodal points is much reduced. Figure 5(c) shows the $\boldsymbol{k}$ space electric intensity profile. There are very few $\boldsymbol{k}_{\measuredangle}$ components inside the leaky region, which accounts for a large $Q_{\perp}$ ($\approx1.9\times10^5$) of this mode.

The effective modal volume for the M0 mode is extremely small, only 2.30 cubic half wavelengths. For a lattice spacing of $450\ nm$, which corresponds to resonant wavelength of $1564\ nm$ for the M0 mode, the modal volume is only $2.76\times10^{-14}\ cm^3$.

#4784 - $15.00 US
Received 12 July 2004; revised 9 August 2004; accepted 10 August 2004

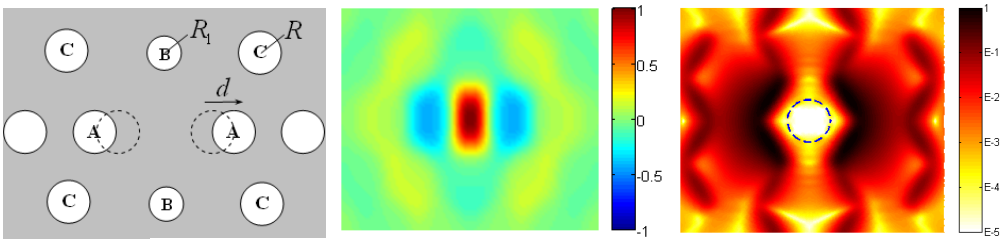

(a) (b) (c)

Fig. 5. (a) M0 cavity, with $d=0.14a$ and $R_1=0.27a$. (b) $\boldsymbol{H}_z$ field distribution of the M0 mode. (c) $\boldsymbol{k}$ space intensity profile I.

For another configuration of the M0 cavity, we set $d=0.14a$ and $R_1=R=0.29a$, that is, we only move 'A' holes outward by $0.14a$, without changing any other surrounding lattice. The modal volume is 2.25 cubic half wavelengths, with $Q_\perp=1.12\times10^5$. Since only the position of two air holes needs to be changed for this modified M0 cavity, without affecting any air hole radius, it is relatively easier to fabricate than other cavities discussed above.

We also calculated the Q value of the other modes supported by the M2, M1 and M0 cavity. The donor modes discussed in this paper have the highest Q value for each cavity respectively.

4. Comparisons

Figure 6 shows the electric field intensity profile for each of the four modes discussed above. From Fig. 6(a) to (d) we can easily see that as the number of missing holes decreases, the electric field intensity maxima in the x direction are pulled closer to each other. The number of nodal points becomes smaller and the field gets more compressed in both x and y directions, leading to reduced modal volumes.

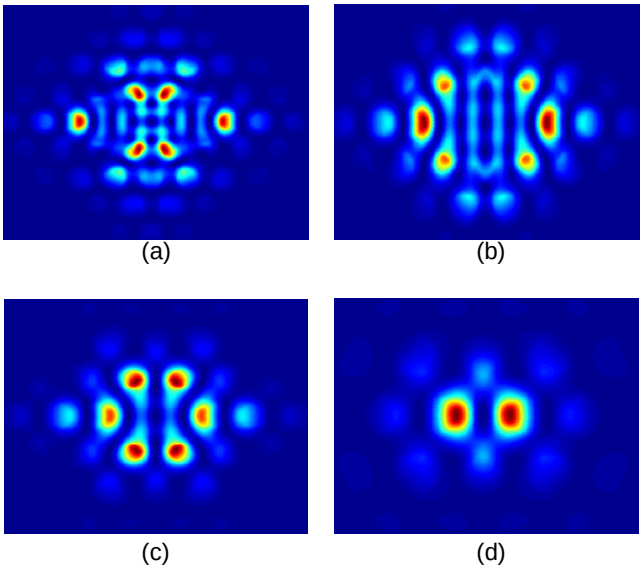

(a) (b) (c) (d)

Fig. 6. Electric intensity distribution of (a) M3 mode, (b) M2 mode, (c) M1 mode, and (d) M0 mode.

Figure 7(a) compares the Q_{tot} value and the effective modal volume of the four modes. We can clearly see that the M1 mode offers the highest Q value and the M0 mode has the smallest modal volume while keeping a relatively large Q. Figure 7(b) compares the $Q_\perp$ and

#4784 - $15.00 US Received 12 July 2004; revised 9 August 2004; accepted 10 August 2004

the radiation factor *RF* of the four modes. $RF = \frac{P}{W}$, where *P* is calculated using equation (3) and (4). *W* is the total energy stored in the cavity [15]. We can clearly see the inverse relation between $Q_{\perp}$ and *RF* in Fig. 7(b).

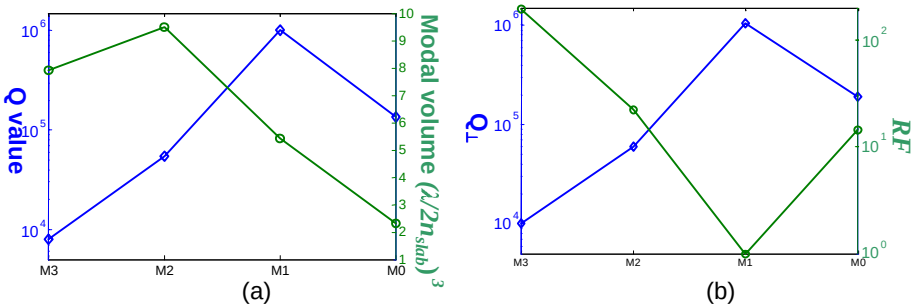

Fig. 7. (a) *Q* value (the blue line with diamond marker) and modal volume (the green line with circle marker) comparison of the four modes. (b) $Q_{\perp}$ (the blue line with diamond marker) and radiation factor *RF* (the green line with circle marker) comparison of the four modes. *RF* is normalized to the M1 mode.

5. Summary

To conclude, we have numerically demonstrated a series of waveguide-section microcavity modes in 2D hexagonal lattice photonic crystal slabs. High *Q* factor larger than 10^6 is obtained for the M1 mode by carefully tuning some structural parameters. Modal volume as small as *2.30* cubic half wavelengths is achieved for the M0 mode. The profile of the M0 mode is simple, yet with *Q* factor exceeding 10^5. We believe that M0 and M1 cavities are well suited for large-scale photonic integration and single-photon sources for quantum optics operations.

Acknowledgments

This work was supported by the Swedish Foundation for Strategic Research (SSF) on Photonics and the Swedish Research Council (VR) under project 2003-5501.

#4784 - $15.00 US Received 12 July 2004; revised 9 August 2004; accepted 10 August 2004